

Chapter 4

Modelling hydrodynamics of Gulf of Kachchh, Goa and Mangalore coastal regions

4.1 Introduction

In chapter 3, the requirement of time series environmental data set in explaining the case of Indian oil sardine larval survival, migration and aggregation is discussed. But, lack of information on the distribution of fish eggs and larvae emphasize the need for data on early life stages of fish, spatially and temporally at high resolution, to demarcate areas of fish abundance. Numerical modelling is an alternate tool to generate environmental and biological datasets, which can be a surrogate for huge data gaps hampering investigations in fisheries biology. Hydrodynamics is the basis for any other processes in the sea, as it explains the forcings required for the processes. The output of hydrodynamic module is given to particle tracking to track the trajectories of particles (larvae) released from a point. Chapters 4 and 5 explain how the numerical modelling results can be used to compare the biological abundance and fish larval transport in three different marine ecosystems namely, the GoK, Mandovi-Zuari and Mangalore. This chapter describes the numerical modelling related to hydrodynamics of the study regions. It includes details of model domain, model set-up, model calibration, sensitivity analysis, model validation for each domain and finally explains the hydrodynamics of each study area which forms the input for studying the larval transport.

4.2 Model set-up

Setting up a model for the simulation of flow needs a suitable computational domain, which permits proper specification of open boundary conditions for water level or fluxes and wind inputs. Bathymetry is specified with respect to Mean Sea Level (MSL). The bed

friction is included by using Manning number and eddy viscosity presented by Smagorinsky constant as described in chapter 2. Mean wind speed and direction is used for the GoK region (Table 2.2) and AWS wind data is used for Goa and Mangalore regions as input parameter (Figure 2.1), assuming that wind speed and direction are uniform over the model area in a given time step. The warm-up period is set for a few minutes at the initial level, and hence the model gets stabilized within a few hours.

4.2.1 Model domain

In the GoK, choice of the model domain was supported by the results of a previous study [Babu et al., 2005] which suggests that eddies near the open boundary of the GoK could possibly reduce the flushing rate, and thus substantially increase the residence time of discharged material in the GoK. Hence, bathymetry was represented using a regular rectangular Cartesian grid with spacing of 500 *m* and was created by extracting depth data from MIKE-CMAP and Naval Hydrographic Office (NHO, Dehra Dun, India) charts. The model domain extends to 180 *km* and 120 *km* in X and Y directions respectively (Figure 1.2).

In the Goa region, two different model domains were set up with coarse and fine resolution rectangular Cartesian grids of 500 *m* * 500 *m* and 50 *m* * 50 *m* spacings, respectively. Bathymetry data has been linearly interpolated to each grid in the model domain. The coarse resolution domain extends 110 *km* and 140 *km* in the X and Y directions, respectively (Figure 1.4). This domain is used for studying the larval dispersion along the coast. However, this coarse domain is inadequate to resolve some specific details at certain areas, especially inside the estuary. Hence, a fine resolution domain, which extends to 13 *km* and 14 *km* in X and Y directions, respectively (Figure 1.4), has been considered to simulate hydrodynamics and larval transport inside the estuary.

For the Mangalore region, the coastal stretch is shorter compared to the previous studies. Hence, a model bathymetry of 200 *m* * 200 *m* regular rectangular Cartesian grid has been created. The model domain extends 65 *km* and 50 *km* in the X and Y directions, respectively (Figure 1.5).

4.2.2 Time step and length of simulation

The time step interval (Δt) for the simulation has been selected in such a way that it should satisfy the stability criterion. The values of Δt and duration of the simulation for the study region are listed below:

- (i) GoK Considering the irregular bathymetry, a time step of 18 s has been selected and this yielded a Courant number of 1.01. Simulations are carried out for a specific period, representing the respective seasons as given below:
 - (a) April 2002 (Pre monsoon)
 - (b) 17 June 2002 to 4 July 2002 (SW monsoon)
 - (c) November 2002 (NE monsoon).
- (ii) Goa: Time steps of 20 s and 15 s were considered in the coarse and fine models, respectively. The corresponding Courant numbers are 3.6 and 1.7, respectively. The higher Δt in the large domain helps to reduce the computational time, as large set of simulations have been setup for larval transport in this domain. The smaller Δt applied in the small domain is primarily to satisfy the stability criterion as the selected grid size is small. Simulations are carried out for three different seasons as given below:
 - (a) December 2006 (NE monsoon)
 - (b) April to May 2007 (Pre monsoon)
 - (c) October 2007 (Post monsoon).
- (iii) Mangalore: Since the coastal stretch is smooth with less obstructions, a time step of 10 s is selected and the corresponding Courant number is 1.14. Model simulations are carried out for three different seasons as given below:
 - (a) December 2006 (NE monsoon)
 - (b) April to May 2007 (Pre monsoon)
 - (c) October 2007 (Post monsoon).

4.3 Model calibration

Model calibration could be carried out by adjusting Manning number, eddy viscosity or wind friction factor. Eddy viscosity, K is an empirical constant that typically ranges between 0.01 and 0.06 [DHI, 2001]. A wind friction value of 0.0026 was applied as a constant in time and space for the model domain. Similar values were followed by the researchers Babu [2005]; Jahfer-Sharif [2009] and Vinod-Kumar [2010] for hydrodynamic model studies along the west coast of India. The details of model calibration are as given below:

4.3.1 Calibration using Manning number

Varying bed resistance has been applied by changing the Manning number (as discussed in chapter 2) to calibrate the model. Thereafter, a uniform Manning number of $32 \text{ m}^{-3} \cdot \text{s}^{-1}$ was applied throughout the GoK domain and this reproduced accurate tide variations all along the GoK. The statistical analysis between modelled and measured water levels and current components at locations off Okha, Mid-channel and Kukadsar yielded a good correlation with less bias (Table 4.1). However, a constant Manning number was not found to be suitable for Goa and Mangalore regions as the simulation blown-up at some of the open boundaries. It has also been found that a Manning number of $32 \text{ m}^{-3} \cdot \text{s}^{-1}$ could not reproduce the accurate tide variations as the bottom features are different from that of GoK. Hence, a variable bed resistance file has been created with low Manning number ($\leq 10 \text{ m}^{-3} \cdot \text{s}^{-1}$) at the open boundaries and high Manning number (25 to $60 \text{ m}^{-3} \cdot \text{s}^{-1}$) at narrow channels according to the bottom roughness of the region. Hence, two different resistance files (calibrated) have been applied for actual simulations in Goa and Mangalore regions. The use of bed resistance file reduced the stability problems and provided better output as seen in the comparisons at Captain of Ports jetty in Goa region and Suratkal in Mangalore region (Table 4.1). Close match and positive correlation ($r \geq 0.43$) between modelled and measured data at different locations across the model domain (Table 4.1) indicate that the model is able to reproduce water level and currents accurately in the entire model domain of respective study area.

Table 4.1 Quality indices used for comparing model results with current measurements and tides at locations along the entire model domain illustrating reproducibility of proper flow fields

Parameter	Location	Component	Bias	RMS	Corr.coeff.
Current speed ($m.s^{-1}$)	Off Okha	u	0.04	0.18	0.87
		v	0.07	0.17	0.91
Water level (m)			0.06	0.39	0.87
Current speed ($m.s^{-1}$)	mid-channel GoK	u	-0.01	0.15	0.98
		v	0.00	0.09	0.09
Water level (m)			0.10	0.50	0.84
Current speed ($m.s^{-1}$)	Off Kukadsar	u	0.08	0.15	0.95
		v	0.06	0.15	0.92
Water level (m)			-2.00	2.08	0.94
Current speed ($m.s^{-1}$)	Captain of Ports jetty	u	0.16	0.37	0.71
		v	-0.06	0.14	0.68
Water level (m)			-0.14	0.15	0.99
Current speed ($m.s^{-1}$)	Off Suratkal	u	-0.01	0.03	0.43
		v	-0.05	0.10	0.65
Water level (m)			0.01	0.02	1.00

4.3.2 Calibration using Eddy viscosity

The Smagorinsky constant is used to damp out numerical oscillations and stabilize the model. The Smagorinsky constant is initially set to $0.4 m^2.s^{-1}$. But, the best fitting of the model simulation to the measured parameters is achieved by setting it to $0.5 m^2.s^{-1}$. Hence, this value has been applied as the calibration factor in actual simulation.

4.4 Model validation for flow pattern

The validation process gives an indication of the model sensitivity and confidence that the results it produced are consistent with measurements. Recording current meter (model: RCM7; make: Aanderaa, Norway) data, measured during the study period, were used for model validation. Comparison between measured and modelled u and v components of the current show good match. The discrepancies may be due to depth-averaged conditions

simulated by the model. The modelled water level at select stations also show very close agreement with the measured/predicted water level, indicating that the model is well calibrated for the study regions (Figures 4.1, 4.2 and 4.3). Scatter plots (Figures 4.4, 4.5 and 4.6) between measured and modelled water level, zonal (u) and meridional (v) currents show that how the model is reasonably reproducing the accurate hydrodynamics of the study regions.

4.4.1 Gulf of Kachchh

Correlation coefficients of 0.59 and 0.54 have been obtained between measured and modelled ebb and flood velocities, respectively. There is slight over-estimation of modelled flow velocities for ebb and flood, with a bias of 0.06 and 0.12 $m.s^{-1}$, respectively. The *R.M.S.* error observed for ebb and flood velocities are 0.18 $m.s^{-1}$ and 0.25 $m.s^{-1}$, respectively. The modelled and predicted water levels show a very good match with no phase difference. Table 2 indicates that the model reproduces water level and currents accurately in the entire model domain. Results show strong u -component and weak v -component in the GoK. Seasonal changes in the flow patterns in the GoK were simulated (Table 4.2) for three different seasons, namely, pre monsoon (April 2002), SW monsoon (June 2002) and NE monsoon (November 2002).

4.4.2 Goa coastal region

Model results have been validated with measurements carried out during 14 November to 10 December, 2007 (Figure 4.2). The modelled and predicted water levels show a very good match with no phase difference. The modelled u and v -velocities show good match with the measured current velocities. Correlation coefficients of 0.71 and 0.68 have been obtained between measured and modelled u and v -velocities, respectively. A slight over-estimation of the modelled u -velocity has been noticed, with a bias of 0.16 $m.s^{-1}$. The modelled v -velocity is slightly under-estimated, with a bias of -0.06 $m.s^{-1}$. The *R.M.S.* error observed for u and v -velocities are 0.37 $m.s^{-1}$ and 0.14 $m.s^{-1}$, respectively.

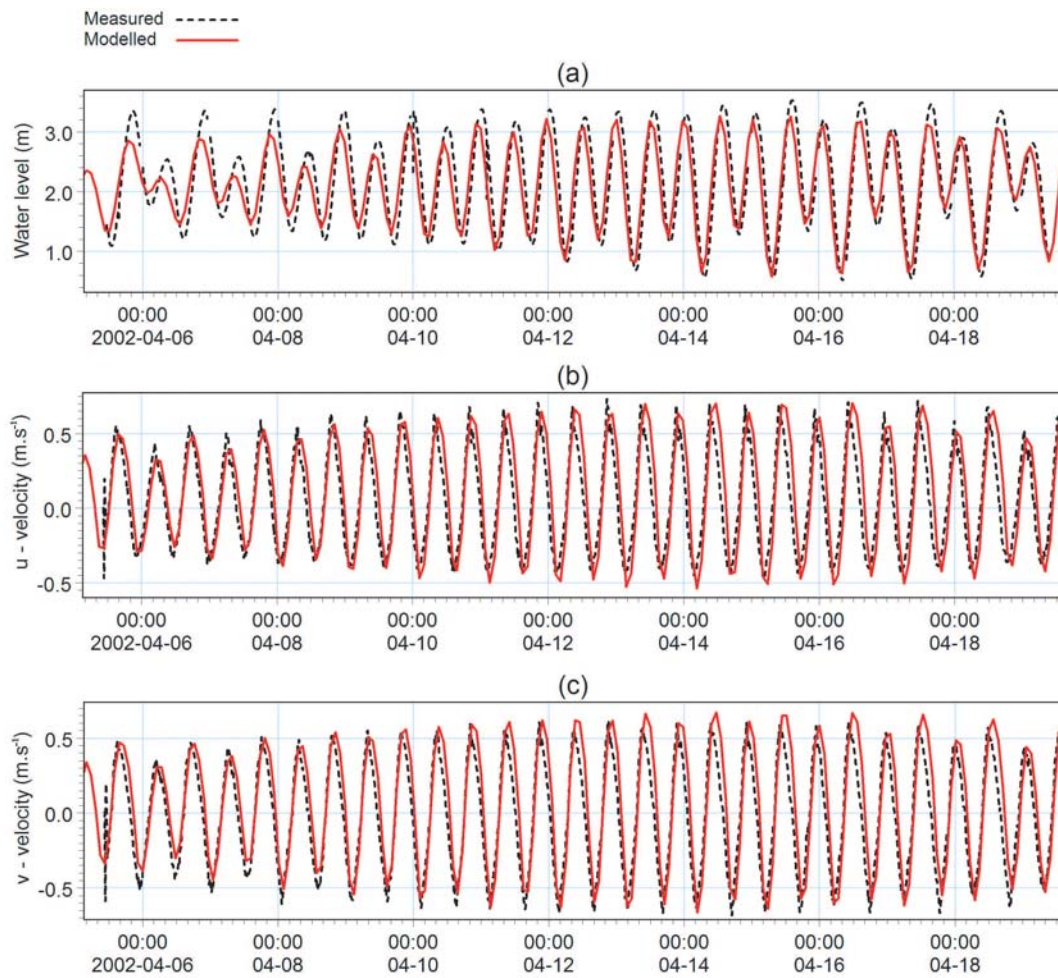


Figure 4.1: Comparison between measured and modelled water level and current off GoK: (a) water level, (b) u velocity and (c) v velocity

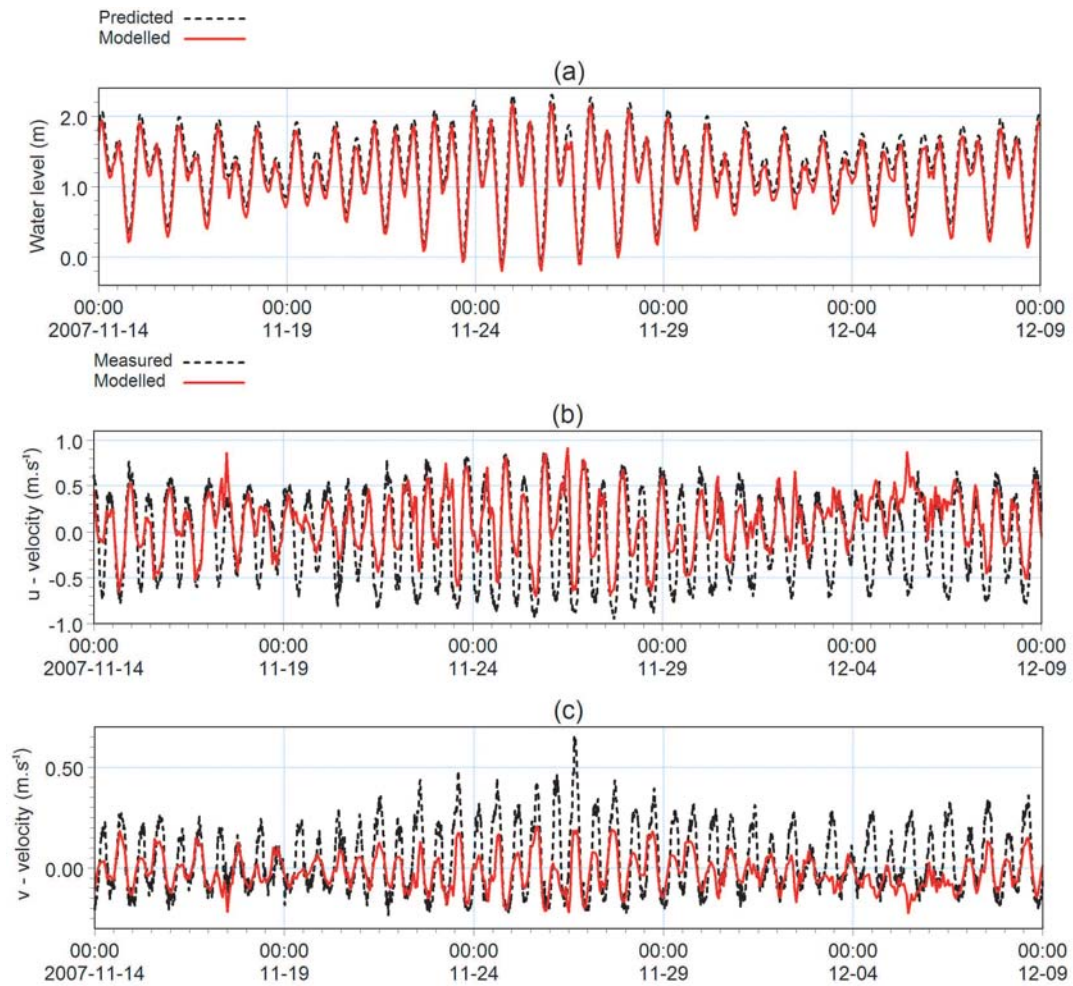


Figure 4.2: Comparison between measured and modelled water level and current off Captain of Ports: (a) water level, (b) u velocity and (c) v velocity

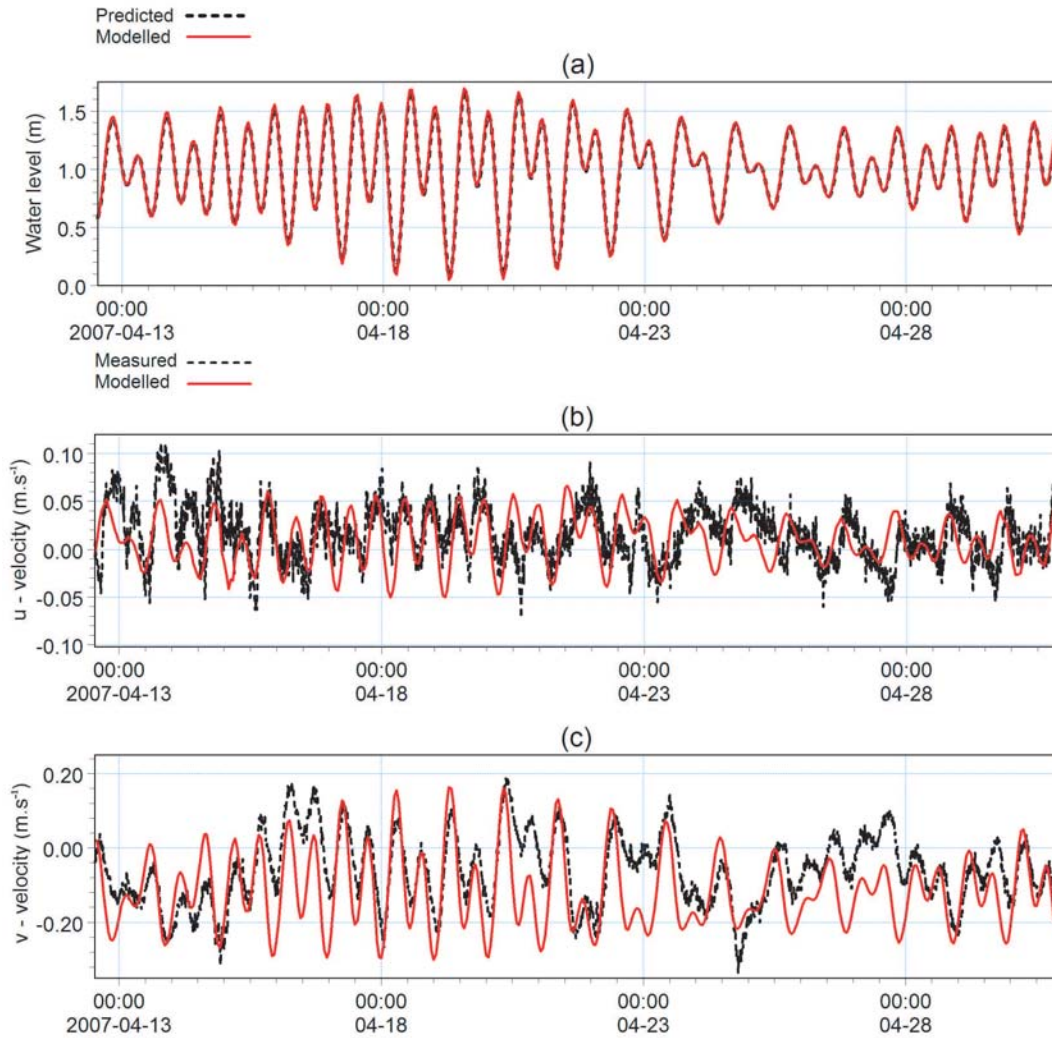


Figure 4.3: Comparison between measured and modelled water level and current off Suratkal: (a) water level, (b) u velocity and (c) v velocity

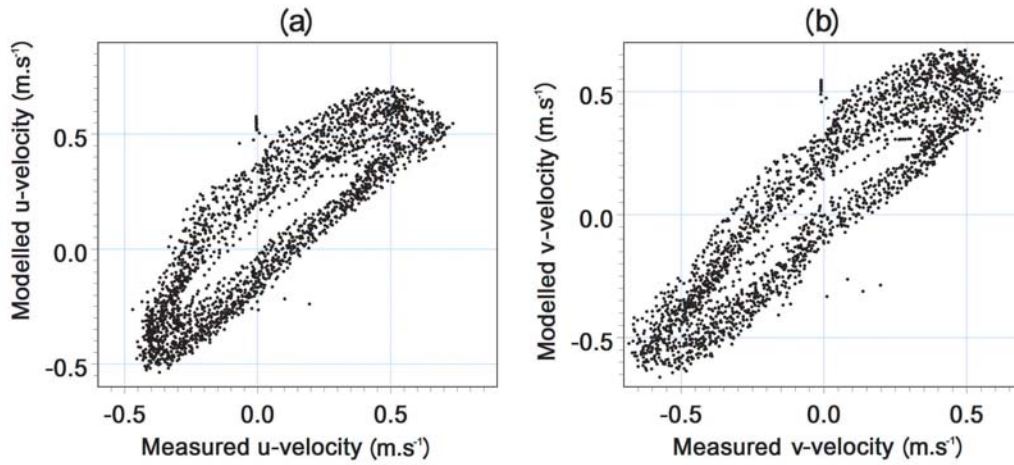


Figure 4.4: Scatter showing measured and modelled currents off Okha: (a) u -velocity and (b) v -velocity

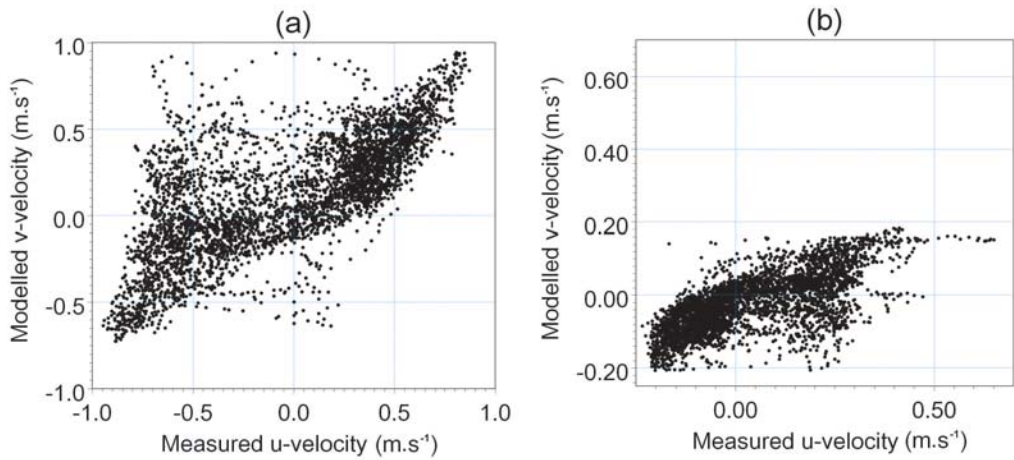


Figure 4.5: Scatter showing measured and modelled currents off Captain of Ports jetty: u -velocity and v -velocity

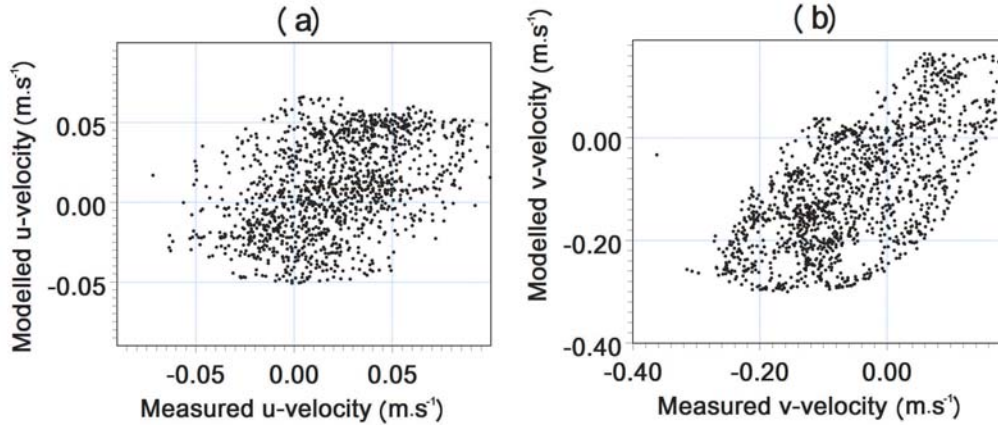


Figure 4.6: Scatter showing measured and modelled currents off Suratkal: u -velocity and v -velocity

4.4.3 Mangalore coastal region

Model results have been validated with measurements carried out during 14 November to 10 December, 2007 (Figure 4.3). The modelled and predicted water levels show a very good match with no phase difference. The modelled u and v -velocities show good match with the measured current velocities. Correlation coefficients of 0.43 and 0.65 have been obtained between measured and modelled u and v -velocities, respectively. A slight under-estimation of the modelled u and v -velocity has been noticed, with a bias of -0.01 m.s^{-1} and -0.05 m.s^{-1} respectively. The *R.M.S.* error observed for u and v -velocities are 0.03 m.s^{-1} and 0.10 m.s^{-1} , respectively.

4.5 Flow patterns in the study regions

Water levels and flow patterns have been analyzed for each study regions for different seasons and the results are discussed below.

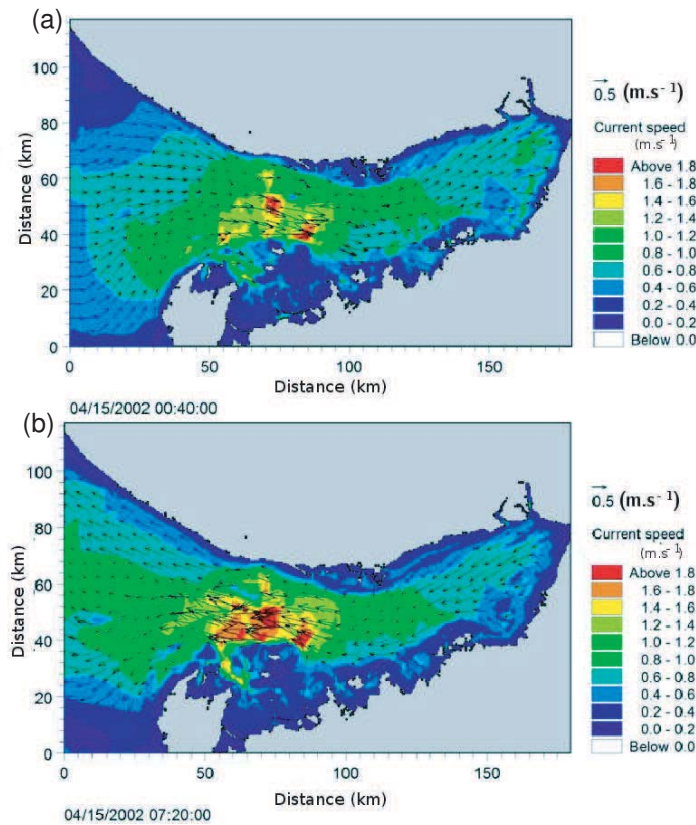


Figure 4.7: Typical current patterns off Okha (April 2002) on a spring tide: (a) during flood and (b) during ebb

4.5.1 Gulf of Kachchh

For the GoK region, the flow pattern during pre monsoon (April 2002), SW monsoon (June 2002) and NE monsoon (November 2002) are simulated and presented (Table 4.2). The model results show that tidal currents control the circulation. The major currents go from the mouth to the head of the Gulf in the ENE direction during flood and WSW during ebb, with relatively high currents along the central Gulf (Figure 4.7). The geometry of the Gulf is such that the entry of water during flood is through the southern side and pushes the water inside. Thereafter, the flow is deflected towards north as the width drops at the mid-Gulf and coastal orientation changes from the mid-Gulf to the head. During ebb the

outward flow is mostly along the northern rim of the Gulf. A cross-section of the flow pattern during different seasons at Okha, mid-channel and Kukadsar (Table 4.2) indicate 50 to 80% higher current speed in the mid-channel compared to Okha (at the Gulf mouth) and Kukadsar (at the Gulf head). The residual velocity is important in understanding the transport of eggs or larvae discharged in a coastal environment. Residual velocity is driven by density gradients and tides. Since the GoK is a well mixed basin, density gradient contribution to the residual current is ignored and tide induced residual currents are analysed. The residual velocity field computed from the model results confirmed the existence of three distinct permanent eddies with diameter varying between 10 and 20 *km* in the western half of the gulf, an anti-cyclonic eddy south of Ranwara shoal, a cyclonic eddy east of it and another anti-cyclonic eddy located between the cyclonic eddy and the investigator reef [Vethamony et al., 2004; Babu et al., 2005]. Thus in the eastern half of the Gulf, the circulation shows a net transport towards Kandla (along the northern rim of the Gulf) which induces the clockwise circulation. On the contrary, in the western Gulf, it is anti-clockwise. It is evident that the net transport from the open ocean into the Gulf is primarily through the southern side of the mouth, and the net outward transport is through the northern side.

Table 4.2 Characteristic flow pattern for different seasons in the GoK

Season	Current	Off Okha		Pre-dominant		Max.current		Mid-channel		Pre-dominant		Max.current		Off Kukadsar				
		speed($m.s^{-1}$) Ebb	Flood	dir($^{\circ}N$) Ebb	Flood	speed($m.s^{-1}$) Ebb	Flood	dir($^{\circ}N$) Ebb	Flood	speed($m.s^{-1}$) Ebb	Flood	dir($^{\circ}N$) Ebb	Flood	speed($m.s^{-1}$) Ebb	Flood	dir($^{\circ}N$) Ebb	Flood	
Pre- monsoon	measured	0.80	0.94	210	210	50	50	1.37	1.35	265	265	90	90	0.86	0.87	235	235	55
SW- monsoon	modelled	0.89	1.06	210	210	45	45	1.63	1.64	265	265	90	90	0.87	0.77	230	230	50
NE- monsoon	measured	0.74	0.99	225	225	45	45	1.06	1.09	275	275	105	105	0.89	1.3	340	340	140
monsoon	modelled	1.4	1.2	260	260	95	95	1.88	1.67	260	260	100	100	1.28	0.91	240	240	55
monsoon	modelled	1.4	1.2	270	270	90	90	1.19	0.94	270	270	105	105	0.81	1.3	340	340	140

No measurements during this season

During pre monsoon, the winds are weak and consistently in the westerly direction. The model simulated tidal currents during spring ebb and flood show an apparent increase in the u component by about 10% in the absence of wind forcing. However, during neap, the tidal currents show a reduction upto 20% compared to the measured currents, suggesting that wind forcing is more effective during neap than spring phase [Vethamony and Babu, 2010].

4.5.2 Goa coastal region

For the Goa region, the flow pattern during NE monsoon (December 2006), pre monsoon (May 2007) and post monsoon (October 2007) are simulated and presented (Table 4.3). The flow along the Goa coast is towards north while flooding and towards south while ebbing, with a prominent southward drift during pre monsoon and NE monsoon seasons. However, during post monsoon season, the prominent drift is towards north. In the Mandovi-Zuari estuarine system, the flow is towards east while flooding and towards west while ebbing. The tidal currents play major role in the cross-shore movement of the particles in the estuarine systems. However, small scale tidal eddies also influence the dispersion characteristics inside the estuary. The flow is relatively higher inside the Mandovi river. The maximum current speeds at the COP while flooding are 0.96, 0.88 and 0.70 $m s^{-1}$ during pre monsoon, post monsoon and NE monsoon seasons, respectively, whereas they are 0.89, 1.08 and 0.65 $m s^{-1}$ respectively, while ebbing. The maximum current speeds inside the Zuari estuary (at the larval sampling point) while flooding are 0.3, 0.63 and 0.12 $m s^{-1}$ during pre monsoon, post monsoon and NE monsoon seasons, respectively, whereas they are 0.33, 0.39 and 0.20 $m s^{-1}$ respectively, while ebbing.

Table 4.3 Characteristic flow pattern for different seasons in the Mandovi estuary

Season	Current	Sampling point (near Dona Paula)				Off Goa				Off COP			
		Max.current speed($m.s^{-1}$) Ebb	Flood	Pre-dominant dir($^{\circ}N$) Flood	Ebb	Max.current speed($m.s^{-1}$) Ebb	Flood	Pre-dominant dir($^{\circ}N$) Ebb	Flood	Max.current speed($m.s^{-1}$) Ebb	Flood	Pre-dominant dir($^{\circ}N$) Ebb	Flood
Pre- monsoon	modelled measured	0.33	0.30	265	110	0.15	0.21	315	135	0.89	0.96	285	105
		No measurements during this season											
Post- monsoon	modelled measured	0.39	0.63	265	115	0.26	0.17	320	120	1.3	0.92	285	115
		No measurements at sampling point and off Goa											
NE- monsoon	modelled measured	0.20	0.12	275	95	0.23	0.25	305	125	0.65	0.70	295	115
		No measurements during this season											

A cross section of current speed and direction show that flood currents from the mouth of the estuaries to the head are relatively stronger at narrow stretches of the estuary (Figure 4.8). During SW monsoon season, currents are influenced by the fresh water discharges and this factor was also taken into account in the model simulation. The Hydrodynamic simulation indicates that the coastal water flows into the estuary from the north and flushes out of the estuary towards the south. At the mouth of the estuary, the northward flow takes a cyclonic reversal and flows again southwards without entering the estuary. Thus in general it can be inferred that the flow is controlled by the semi-diurnal tides and reversing seasonal wind patterns to a greater extent. There is an effect of the sea breeze too in the circulation process. The current movement is faster in the narrow channels of the estuarine head. The freshwater influx makes it a fresh water pool in the upstream of the estuary during the SW monsoon and practically remains sea water for the rest of the season in the downstream.

4.5.3 Mangalore coastal region

For the Mangalore region, the flow pattern during NE monsoon (December 2006), pre monsoon (May 2007) and post monsoon (October 2007) are simulated and presented (Table 4.4). Tidal currents are significant in this region. The current speed during ebb tide

Table 4.4 Characteristic flow pattern for different seasons in Mangalore region

Season	Current	Off Mulki				Off Suratkal			
		Max.current speed(ms^{-1})		Pre-dominant dir($^{\circ}N$)		Max.current speed(ms^{-1})		Pre-dominant dir($^{\circ}N$)	
		Ebb	Flood	Ebb	Flood	Ebb	Flood	Ebb	Flood
Pre-monsoon	measured	No measurements off Mulki				0.40	0.30	170	360
	modelled	0.13	0.19	335	165	0.30	0.17	180	350
Post-monsoon	measured	No measurements during this season							
	modelled	0.14	0.28	335	160	0.30	0.17	180	350
NE-monsoon	measured	No measurements during this season							
	modelled	0.17	0.41	330	160	0.28	0.29	180	90

is stronger than the flood tide since the wind driven currents are also in the same direc-

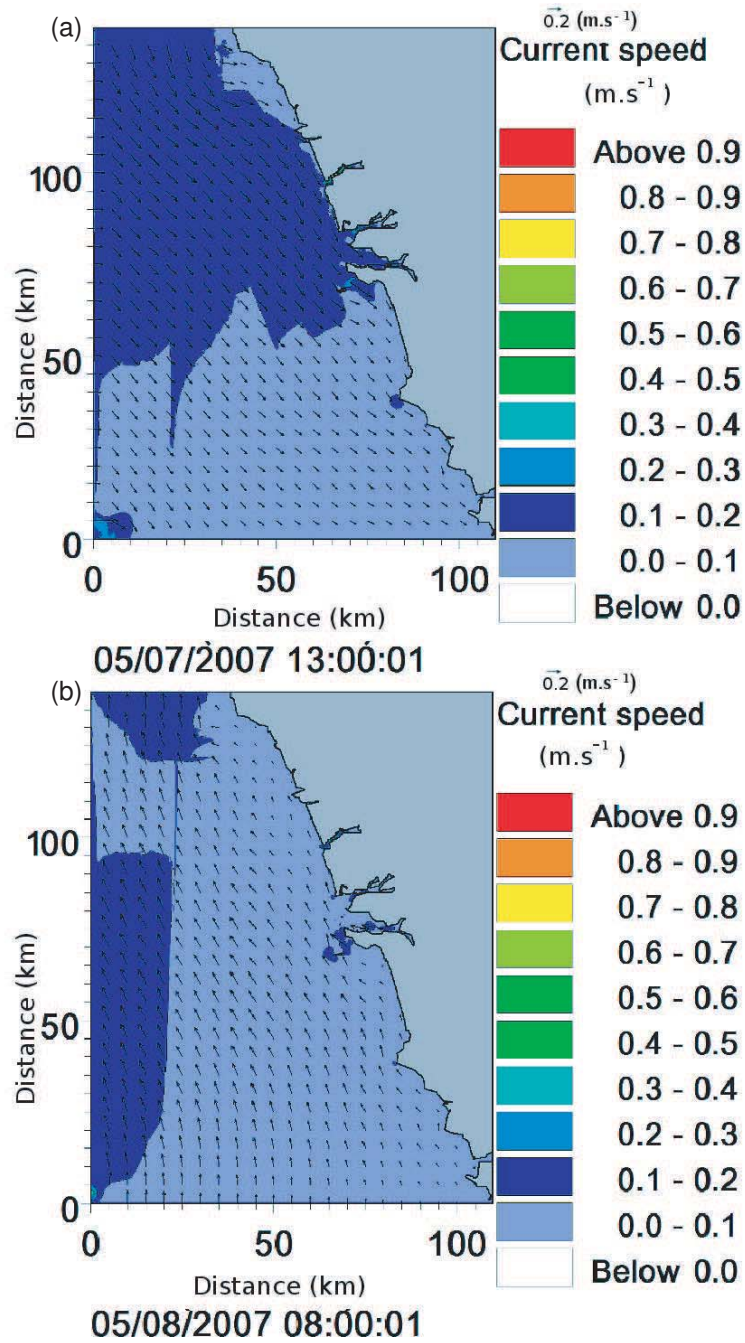


Figure 4.8: Typical current patterns in the Mandovi-Zuari during (April 2006) on a spring tide: (a) during flood and (b) during ebb (

tion. During ebb tide, the predominant flow is towards south and during flood the flow is towards north. Tidal currents oscillate mainly in the longshore direction with little net cross-shore current. The onshore and offshore currents (u -component) were meager compared to the alongshore currents (v -component), irrespective of the period of simulation. The current slows down during the tidal slack, that is, just before current reversal takes place. There will be no contribution by the fresh water discharges during NE monsoon period, but we can expect some contribution during SW monsoon period, but that will be very minimal. The simulated current shows that the currents are having distinct variability corresponding to the tide. In general, the current speed remains low $\leq 0.3 \text{ m.s}^{-1}$ usually, except during spring tide when current speed reaches a range of $0.5\text{-}0.7 \text{ m.s}^{-1}$ at the narrow estuarine mouth of River Netravati (Figure 4.9). The simulations indicate that the orientation of the main axis of the current flow as NW-SE during both the seasons. The current vectors were also split into N-S and E-W components (Figure 4.9). The N-S components were influenced by tides. They oscillated with a semi-diurnal frequency. The E-W components were affected mostly by winds. The eastward component was comparatively stronger than the westward component. The coastal flow off Mangalore could be considered as reversing tidal currents flowing more or less parallel to the coast with an onshore drift under the influence of the existing wind pattern.

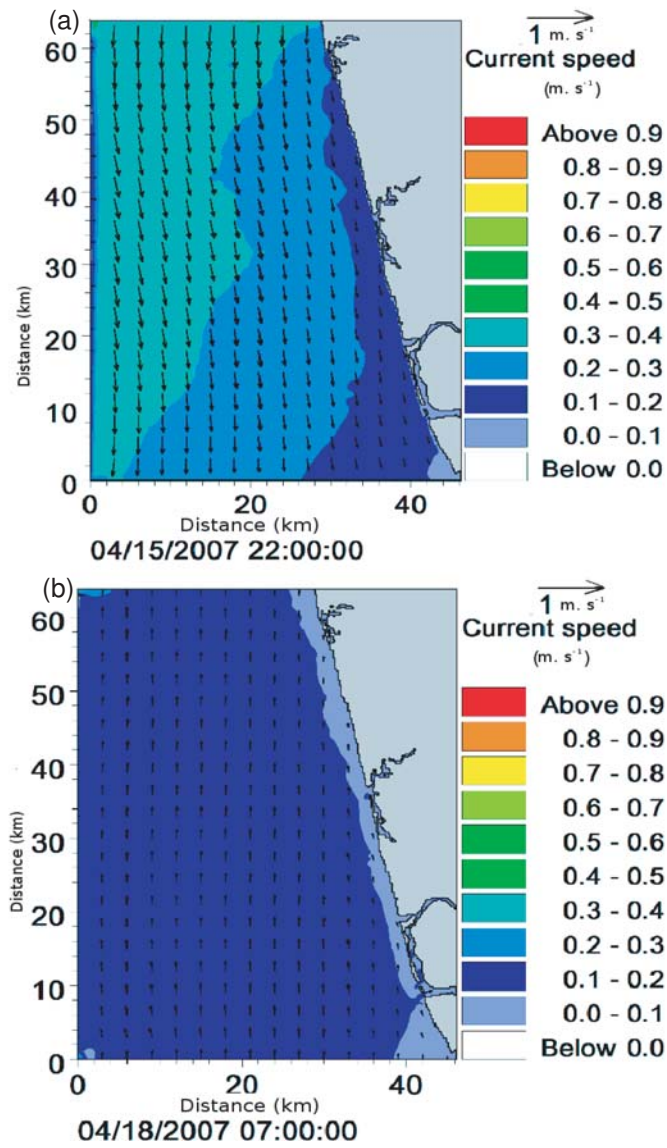


Figure 4.9: Typical current patterns off Mangalore (April 2006) on a spring tide: (a) during flood and (b) during ebb